

TEMPERATURE VARIATION EFFECT ON THE ACTIVE VIBRATION CONTROL OF SMART COMPOSITE BEAM

Mostefa SALAH,* Farouk B. BOUKHOULDA,* Mohamed NOUARI, Kouider BENDINE***

*Structures and Solid Mechanical Laboratory, Mechanical Department, Djillali Liabes University of SidiBel- Abbes,
BP 89 Cité Ben M'Hidi Sidi Bel-Abbès 22000, Algérie.

**University of Lorraine, Laboratoire d'Etude des Microstructures et de Mécanique des Matériaux,
LEM3 CNRS-UMR 7239, GIP-INSIC, 27 Rue d'Hellieule, 88100 Saint-Dié-des-Vosges, France.

mostefa.salah@yahoo.fr, boukhoulde22000@yahoo.fr, nouari.mohamed@univ-nancy.fr, bendine.k@live.fr

received 14 January 2020, revised 17 November 2020, accepted 19 November 2020

Abstract: Due to their impressive capacity of sensing and actuating, piezoelectric materials have been widely merged in different industrial fields, especially aeronautic and aerospace area. However, in the aeronautic industry, the structures are operating under critical environmental loads such as high and very low temperature, which made the investigation of the effect of thermal forces on the piezoelectric structures indispensable to reach the high functionality and performance. The present paper focuses on the effect of thermal loads on the active vibration control (AVC) of structures like beams. For this purpose, a finite element model of composite beam with fully covered piezoelectric sensor and actuator based on the well-known high order shear deformation theory is proposed by taking into account the electrical potential field and a linear temperature field. Hamilton's principle is used to formulate the electro-thermo-mechanical governing equations. The negative velocity feedback controller is implemented to provide the necessary gain for the actuator. Different analyses are effectuated to present the effect of the temperature ranging from -70°C to 70°C on the active vibration control of the composite beam.

Keywords: Piezoelectric, thermal loads, beams, active vibration control, Hamilton's principle

1. INTRODUCTION

Structures made of composite materials are intensively used in different industrial sectors (Gay and Hoa, 2007). Due to their light weight, rigidity and high physical properties, they can be found especially in aeronautic and aerospace technology. These structures are subjected to different type of critical loads, which lead to huge amount of vibrations. The vibrations are mostly undesirable and significantly affect the composite structures and cause their failure and damage (Zou et al., 2000). To prevent the failure of the composite structures caused by the vibration, the research community proposed a variety of solutions, among them passive, semi active and active vibration control. The passive damping techniques (PDT) (Johnson, 1995) is based on the integration and the addition of materials or systems, possessing high damping properties, into the structure in such a way that the vibrations can be absorbed by the developed damping system without any further outside interference. However, these techniques have certain limitations: their performance is limited in the low frequency domain, the size can be important and the damping coefficient is especially dependent on temperature and frequency. Semi-active control methods are well known in the context of structural vibration using piezoelectric actuator to dissipate energy caused by the system's motion (Clark, 1999). The main benefit is that no additional energy is added to the system, and their implementation does not require any sophisticated signal processing systems or any bulky power amplifier (Qiu et al., 2009), which guarantees stability of the whole system. In addition, semi-active methods are more efficient than the passive ones, but always with

a lower efficiency in comparison to the active methods. The last technique, which is the main objective of this study, is the based on piezoelectric active vibration control (AVC). It is inspired by the phenomena of piezoelectricity in certain materials (Ye, 2008), the AVC techniques are gradually merged in different fields (Crawley and De Luis, 1987). It consists of four main keys, the structure itself, the sensor, the actuator and the control algorithms. Thus, it requires bonding piezoelectric patches in a conventional structure to create a kind of smart structure, which have the ability of self-control.

An explosion of research papers have been focused on the finite element modelling of the AVC using piezoelectric materials. Lam et al. (1997) developed a finite element model for piezoelectric composite laminate based on the classical plate theory. Peng et al. (1998) introduced a finite element model using the well-known third order laminate theory for the active vibration control of composite beams with distributed piezoelectric sensors and actuators. Elshafei and Alraies (2013) suggested a finite element formulation for modelling and analysis of isotropic as well as orthotropic composite beams with distributed piezoelectric actuators subjected to both mechanical and electrical loads. Bendine et al. (2016) proposed a finite element method (FEM) to study the active vibration control smart FGM beam based on higher-order shear deformation theory, the authors analyzed different types of loading and provided a displacement feedback controller to reduce the vibrations. Beheshti-Aval et al. (2011) introduced a three noded beam finite element of composite laminated beam with distributed piezoelectric sensor/actuator layers for the static analysis. Kargarnovin et al. (2007) considered a simply supported

FGM plate bonded with piezoelectric patches; the model equation of motion is derived using classical laminated plate theory CLPT. Tzou and Tseng (1990) derived a new piezoelectric finite element with internal degree of freedom for modelling a shell or plate structures containing distributed piezoelectric sensor and actuator. Tzou and Gadre (1989) established an experimental work to model active vibration suppression of a multi-layered shell coupled with piezoelectric actuators.

Otherwise, the composite structures are used under a high critical environmental thermal field, especially in aerospace sector. This variation in temperature effects the system performance and, in particular, their dynamic responses. Recently, a great number of researches have focused on the analysis of piezothermoelasticity. Lee and Saravanos (1996) developed and implemented a finite element equation to a beam element with linear shape function to model mechanical, electrical and thermal responses of composite beam integrated with piezoelectric patches. Zhou et al. (2000) used a higher order temperature field to describe the temperature distribution through the thickness of a composite plate; a thermo-piezoelectric-mechanical theory is adopted to model dynamic response of a composite plate bonded with piezoelectric actuator. Bansal and Ramaswamy (2002) investigated the dynamic as well as static thermal responses of laminated composites bonded with piezoelectric layers by using a four node finite element formulation, which have five mechanical degrees of freedom per node. Lee and Saravanos (1998) implemented finite element equations for beams and plates to model active response of piezoelectric composite laminate taking into account the thermal effect on the material properties. Liew et al. (2001) presented a finite element formulation to model active control of functionally gradient material FGM plate integrating with piezoelectric layers, the model is based on the first shear deformation theory and he subjected to a thermal gradient. Jiang and Li (2007) used a negative velocity feedback for active vibration control of a composite beam distributed with piezoelectric sensor and actuator layers subjected to a thermal excitation, the finite element model is based on a high-order displacement field. Raja et al. (2004) derived the finite element actuator and sensor using a nine noded field consistent shallow shell element to analyze piezohygrothermoelastic laminated plates and shells. Gupta et al. (2011) introduced AVC of a smart cantilever plate using negative velocity feedback control at elevated temperature ranging from 25°C to 75°C. Sharma et al. (2016) investigated the dynamic response and the AVC of cantilever structure over a temperature range (-70°C–70°C) experimentally and numerically, the model is based on the first order shear deformation theory. Song et al. (2004) presented a numerical and experimental study of active reduction of deformation due to thermal effect of a composite beam using piezoelectric ceramic actuators. Birman (1996) studied the effect of temperature on piezoelectric sensors and on a composite layer. Chandrashekhara and Tenneti (1995) developed an FEM for the active control of thermally induced vibration of laminated composite plate bonded with piezoelectric actuators. Chattopadhyay et al. (1999) applied the principle of free energy and Hamilton's principle to obtain differential equations to modelling a coupled thermo-piezoelectric-mechanical of composite laminate bonded with piezoelectric actuators in the surface.

In the previous paper, the piezoelectric coefficients' values were assumed to be independent of temperature, which is not correct. The present paper proposes a finite element formulation of composite beam based on the well-known high order shear deformation theory. The piezoelectric coefficients were supposed

to be dependent on temperature. Two types of analysis are considered, which include static and dynamic responses. A negative velocity feedback algorithm is used to provide the necessary gain for the active vibration control of the composite beam. Different results are presented to prove the efficiency of the proposed model.

2. HAMILTON'S PRINCIPLE

As presented in Fig. 1, a laminated beam with two piezoelectric films bounded on its top and bottom surfaces is considered in this study. To derive the structure thermoelectromechanical equations, the well-known Hamilton's principle, which assumes that the energy variation over an arbitrary period of time equals zero, is used.

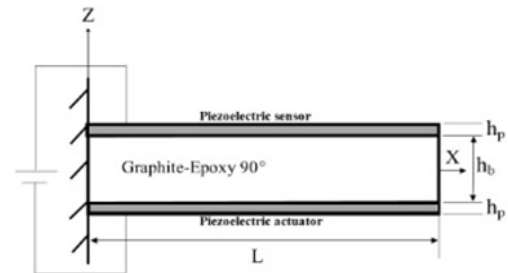


Fig. 1. Cantilever graphite-epoxy Beam (90°) distributed with piezoelectric patches

The mathematical statement of Hamilton's principle, which explains the variation of integration of the total energy, can be expressed as follows:

$$\int_{t_1}^{t_2} \delta(T - P) dt = 0 \quad (1)$$

where T and P are respectively the kinetic and the potential energies of the structure that can be defined as (Tzou and Bao, 1995):

$$T = \int_V \left(\frac{1}{2} \rho \dot{u} \dot{u} \right) dv \quad (2)$$

$$P = \int_V [M(\sigma_i, E_j, \theta_a) + \Omega \theta_a] dv - \int_S [s_j u - q_j \lambda] ds \quad (3)$$

We noted here that u and \dot{u} are the displacement and velocity, σ_i , E_j are the strain and the electric field, θ_a is the absolute temperature and Ω is the thermal entropy density, ρ , M and q_i is the mass density, the electric enthalpy and the surface electric charge, s_j is the surface traction in the J direction and λ is the electrical potential. V and S are the volume and surface of the piezothermoelastic continuum.

The electric enthalpy M can be formulated as:

$$M = \frac{1}{2} \{\sigma\}^t [C] \{\sigma\} - \frac{1}{2} \{E\}^t [d] \{E\} - \frac{1}{2} a \theta^2 - \{E\}^t [p] \{\sigma\} - \{\chi\}^t \{\sigma\} \theta - \{\kappa\}^t \{e\} \theta \quad (4)$$

where $\{\sigma\}$, $\{E\}$, $\{\chi\}$ and $\{\kappa\}$ denote respectively strain vector, electric field, stress temperature and pyroelectric coefficient vector

and $[C]$, $[d]$ and $[p]$ represent lastic stiffness, dielectric permittivity and piezoelectric coefficient matrix.

We noted that θ is the temperature rise and α_v is a material coefficient done by $\alpha_v = \rho c_v \theta_0^{-1}$, where c_v is the specific heat and θ_0 is the temperature of the natural plane.

Using Eq. (2) and (3) and including the electric enthalpy formula Eq. (4), the Hamilton's equation for the laminated piezoelectric beam can be rewritten as:

$$\int_{t_0}^{t_1} \int_v \frac{1}{2} \rho \delta(u)^2 dV dt - \int_{t_0}^{t_1} \int_v \{D\}^t \Delta(\delta\lambda) + \{S\}^t \delta\{\sigma\} dV dt + \int_{t_0}^{t_1} \int_v (t_f \delta u_f - q_j \delta \lambda) dS dt = 0 \quad (5)$$

3. PIEZOTHERMOELASTIC CONSTITUTIVE EQUATIONS

According to Benjeddou and Andrianarison (2005), the piezothermoelastic field, which is by definition the elasto-electric-thermal interactions, is given by:

$$\begin{aligned} \{S\} &= [C]\{\sigma\} - [p]^T\{E\} - \{\chi\}\theta \\ \{D\} &= [p]\{\sigma\} + [d]\{E\} + \{\kappa\}\theta \\ \Omega &= \{\chi\}\{\sigma\} - [\kappa]^T\{E\} + a\theta \end{aligned} \quad (6)$$

It must be noted that $\{S\}$, $\{D\}$ and Ω are respectively the stress, electric displacement and thermal entropy density vector.

4. DISPLACEMENT AND STRAIN

According to Reddy (1984) and Zorić et al. (2013) and based on a simple higher-order shear deformation theory, the displacement field can be written as following (Eq. 7):

$$\begin{cases} u(x, z, t) = u_0(x, t) - z \frac{dw(x)}{dx} + (z - z^3 \frac{4}{3h^2}) \varphi_x(x, t) \\ w(x, z, t) = w_0(x, t) \end{cases} \quad (7)$$

where: (u, w) and (u_0, w_0) are the displacements of any point and the mid-plane displacement in the x and z directions. φ_x is the bending rotation of the mid-plane and h is the total thickness of the composite structure.

From Eq. (7), the strain equation can be derived as:

$$\begin{cases} \sigma_1 = \sigma_x = \frac{du}{dx} - z \frac{d^2w(x)}{dx^2} + (z - z^3 \frac{4}{3h^2}) \varphi_x(x, t) \\ \sigma_5 = \tau_{zx} = (z - z^3 \frac{4}{3h^2}) \varphi_x(x, t) \end{cases} \quad (8)$$

We noted here that τ is the shear strain. The strain and displacement Eq. (9) and (10) can be presented as:

$$u = a_u u_u \quad (9)$$

$$\varepsilon = l_u u_u \quad (10)$$

where:

$$a_u = \begin{bmatrix} 1 & -z \frac{d}{dx} & z - \frac{4z^3}{3h^2} \\ 0 & 1 & 0 \end{bmatrix} \quad (11)$$

$$l_u = \begin{bmatrix} \frac{d}{dx} & -z \frac{d^2}{dx^2} & z - \frac{4z^3}{3h^2} \\ 0 & 0 & 1 - \frac{4z^2}{h^2} \end{bmatrix} 0$$

and,

$$\Omega = z^3 - \frac{4}{3h^2} \quad (12)$$

$$\varepsilon_{xx} = \varepsilon_{xx}^0 + z \varepsilon_{xx}^1 - \Omega \varepsilon_{xx}^3 \quad (13)$$

$$\tau_{xz} = \tau_{xz}^0 - z^2 \frac{4}{h^2} \tau_{xz}^2 \quad (14)$$

5. FINITE ELEMENT FORMULATION

5.1. Mechanical field

In this work, the composite structure is modeled using the finite element method. Each beam element has two nodes with four mechanical degrees of freedom $\{u_e\} = \{u, w, \varphi_x, \frac{\partial w}{\partial x}\}$ at each node. One electric degree of freedom for each piezoelectric layer is also used. The axial displacement u and the rotation φ_x are expressed in the nodal displacement in the finite element model as follows (Zorić et al., 2013):

$$\xi_1 = (1 - \gamma)/2 \quad (15)$$

$$\xi_2 = (1 + \gamma)/2$$

where ξ_1 is the Lagrangian shape function.

The transverse displacement w is expressed in the finite element model by a Hermite cubic interpolation shape functions:

$$\begin{aligned} \theta_1 &= 1/4(1 - \gamma)^2 (2 + \gamma) \\ \theta_2 &= 1/4(2 - \gamma)(1 + \gamma)^2 \\ \theta'_1 &= 1/4(1 - \gamma)^2 (1 + \gamma) \\ \theta'_2 &= -1/4(1 - \gamma)(1 + \gamma)^2 \end{aligned} \quad (16)$$

where γ is the local coordinate define as:

$$\gamma = 2 \frac{x}{l_e} - 1 \quad (17)$$

Putting Eq. 15, 16 and 17 into matrix form yields:

$$n_u = \begin{bmatrix} \xi_1 & 0 & 0 & 0 & \xi_2 & 0 & 0 & 0 \\ 0 & \theta_1 & 0 & \theta'_1 \left(\frac{l_e}{2}\right) & 0 & \theta_2 & 0 & \theta'_2 \left(\frac{l_e}{2}\right) \\ 0 & 0 & \xi_1 & 0 & 0 & 0 & \xi_2 & 0 \end{bmatrix} \quad (18)$$

The displacement vector and the strain vector can be expressed as follows:

$$u = a_u u_u = a_u n_u u_u^e = n u_u^e \quad (19)$$

$$\varepsilon = l_u u_u = l_u n_u u_u^e = b_u u_u^e \quad (20)$$

where n is the displacement interpolation matrix and b_u is the strain interpolation matrix.

5.2. Electric field

The electric potential along the k th piezoelectric layer is assumed to be a cubic form, and may be presented as:

$$\phi^k(x, y, \tilde{z}) = p_1^k(\tilde{z})E_1^k(x, y) + p_2^k(\tilde{z})E_b^k(x, y) + p_3^k(\tilde{z})\phi^k(x, y) \quad (21)$$

where: $e_1^k(x, y)$, $e_b^k(x, y)$ are the electric fields at the top and the bottom surface. $\phi^k(x, y)$ is the difference in potential between the top and bottom surface. p_1^k, p_2^k and p_3^k are the interpolation functions that can be given by:

$$\begin{aligned} p_1^k &= -\left(\tilde{z} + \frac{1}{2}\right)^2 \left(\tilde{z} - \frac{1}{2}\right) h_k \\ p_2^k &= -\left(\tilde{z} + \frac{1}{2}\right) \left(\tilde{z} - \frac{1}{2}\right)^2 h_k \\ p_3^k &= 3\left(\tilde{z} + \frac{1}{2}\right)^2 - 2\left(\tilde{z} + \frac{1}{2}\right)^3 - \frac{1}{2} \end{aligned} \quad (22)$$

It is to be noted that h_k and \tilde{z} are the thickness of the k th piezoelectric layer and the local thickness coordinate of the k th piezoelectric layer respectively, $\tilde{z} \in [-1/2 \rightarrow 1/2]$

$$\tilde{z} = \frac{z}{h_k} - \frac{z_t^k z_b^k}{2h_k} \quad (23)$$

z_t^k and z_b^k are respectively the z -axis coordinate for the top and bottom surfaces of the k th piezoelectric layer. The electric field vector E_k for each layer is by definition the gradient of the electric potential, thus, the electric field can be formulated as follow:

$$\begin{aligned} E_k &= \begin{bmatrix} E_x \\ E_z \end{bmatrix} = \begin{bmatrix} -\frac{\partial \phi}{\partial x} \\ -\frac{\partial \phi}{\partial z} \end{bmatrix} \\ &= -\begin{bmatrix} p_1^k \frac{d}{dx} & p_2^k \frac{d}{dx} & p_3^k \frac{d}{dx} \\ \frac{dp_1^k}{dz} & \frac{dp_2^k}{dz} & \frac{dp_3^k}{dz} \end{bmatrix} \begin{bmatrix} E_t^k \\ E_b^k \\ \phi^k \end{bmatrix} = -I_\phi^k U_\phi^k \end{aligned} \quad (24)$$

It is worth to be noted that the potential in the y direction can be taken as $E_y = 0$.

5.3. Thermal field

Assuming that the temperature field is a linear function through the thickness of the beam, hence, the temperature field can be interpolated as:

$$\theta(x, z) = \left(\frac{1}{2} - \frac{z}{h}\right)\theta_b(x) + \left(\frac{1}{2} + \frac{z}{h}\right)\theta_t(x) = B_\theta \theta \quad (25)$$

where θ_t and θ_b are the top and bottom surface temperature, B_θ is the linear interpolation vector for the temperature variation.

6. GOVERNING EQUATION

With the help of Eq. 6, 7, 8, 9 and using Eq. 5, 10 and 11 and taking into account the damping effect, we get the dynamic matrix

equations as follow:

$$m\ddot{u}_u + C_{uu}u_u + C_{ua}u_a + C_{us}u_s = f_u + k_{u\theta}\theta \quad (11)$$

$$K_{au}u_u - e_{aa}u_a = -f_a - k_{a\theta}\theta \quad (12)$$

$$K_{su}u_u - e_{ss}u_s = -f_s - k_{s\theta}\theta \quad (128)$$

where m , C_{uu} , C_{ui} and $k_{u\theta}$ are respectively the mass, the elastic, the matrix coupling electric-mechanical for actuator and sensor and the matrix coupling thermal-mechanical, and e_{aa} , $k_{k\theta}$, f_u and f_s are the permittivity matrix for actuator and sensor, the matrix coupling electric-thermal for actuator and sensor, the mechanical load vector and the applied charge vector; which are of the form:

$$m = \int_v \rho n^t n dv \quad (139)$$

$$C_{uu} = \int_v b_u^t C b_u dv \quad (30)$$

$$C_{ui} = \int_v b_u^t \sigma^t b_\phi dv ; i = (c, a) \quad (31)$$

$$k_{u\theta} = \int_v b_u^t \chi b_\theta dv \quad (32)$$

$$C_{kk} = \int_v b_\phi^t d_k b_\phi dv ; k = (c, a) \quad (33)$$

$$k_{k\theta} = \int_v b_\phi^t \kappa_k b_\theta dv ; k = (c, a) \quad (34)$$

$$f_u = \int_v n^t f_b dV + \int_{S_f} n^t f dS + n^t f_c \quad (35)$$

$$f_k = \int_v n_\phi^t f_k^t q ds ; k = (c, a) \quad (36)$$

6.1. Negative velocity feedback strategy

It should be noted that in this study, we introduce a controller to damp the vibrations caused by the external excitation. A negative velocity feedback controller is considered in order to have good stability and robustness properties. The electrical potential is to be the feedback to the actuator, and is calculated as:

$$\{V\}_a = G_v \{V\}_s \quad (14)$$

where G_v is the control gain.

7. RESULTS AND DISCUSSION

In order to validate the present FE model, a benchmark cantilever beam bonded by piezoelectric along the upper and bottom surface as shown in Fig. 1 is proposed. The beam dimensions

are: length $L = 0.5$ m, with 0.1 m and thickness $h = 0.001$ m. The FEM model is composed of four layers, the stacking sequence is

$[90^\circ/90^\circ/90^\circ/90^\circ]$. The material properties of the structure are listed in the Table 1.

Tab. 1. Material proprieties(Jiang and Li, 2007)

Proprieties	Graphite-Epoxy	PZT
Poisson's ratio $\nu_{12}=\nu_{13}=\nu_{23}$	0.33	0.33
Density $\rho(kg/m^3)$	1600	7750
Elastic stiffness matrix $E(GN/m^2)$	$E_{11} = 180, E_{22} = E_{33} = 10$	$E_{11} = E_{22} = E_{33} = 60,$
Shear modulus $G(GN/m^2)$	$G_{11} = G_{13} = 8, G_{23} = 3,$	$G_{11} = G_{13} = G_{23} = 22.5$
Thermal expansion A	$A_1 = 2.4 \times 10^{-8}, A_2 = A_3 = 2.4 \times 10^{-5}$	$A_1 = A_2 = A_3 = 1.2 \times 10^{-6}$
Electric permittivity $d(F/m)$	--	$d_{11} = d_{22} = d_{33} = 150 \times 10^{-10}$
Piezoelectric strain matrix e	--	$e_{31} = 6.5, e_{33} = 23.3, e_{15} = 17$
Piezoelectric compliance $d(C/N)$	--	$d_{15}=d_{24} = 6 \times 10^{-10},$ $d_{31} = d_{32} = -1.7 \times 10^{-10}$ $d_{33} = 3.5 \times 10^{-10}$
Pyroelectric constant $\kappa(c/km^2)$	--	$\kappa_3 = -2.5 \times 10^{-5}$

Two cases are considered to validate the proposed model. the first case, the beam has been subjected to a temperature gradient of 5, 10, 20 and 50°C, as shown in Fig. 2, the deflection is upwards and proportional to the temperature, which is quite normal due to the fact that temperature in the bottom is higher than the top surface. The results are validated using the study of Jiang and Li (2007).

The second validation case seeks the effect of pyroelectric and thermal strain effect, as shown in Fig. 3; the thermal strain effect is much more significant than the pyroelectric effect. Those results are confirmed by the study of Jiang and Li (2007).

7.1. Temperature effect on the active vibration control

In the area of active vibration control, most research papers consider that the piezoelectric stress coefficients and permittivity are independent of the temperature, which is quite incorrect due to the fact that the coefficients are highly sensitive to the temperature and their change can be described as linear when it comes to the stress coefficients and nonlinear for the case of permittivity (Gupta et al., 2011). In the present work, we considered the variations in piezoelectric and permittivity coefficients versus the temperature in the bandwidth of $[-70^\circ C$ to $+70^\circ C]$ for the case of lead zirconate titanate ceramic PZT-5H, which are provided by the experimental investigation done by Wang et al. (1998), which is shown in Table 2.

Tab. 2. Dielectric constant and permittivity coefficient of piezo-electric materials versus temperature (Sharma et al., 2016)

Temperature ($^\circ C$)	Piezoelectric constant (d_{31}) 10^{-12} (pC/N)	Dielectric constant (k_{33}) 10^{-9} (F/m)
-70	1.6	1.67
-50	1.84	1.92
-25	2.13	2.22
0	2.43	2.49
25	2.72	2.84
50	3	3.11
70	3.24	3.34

To study the performance of the active vibration control under the aforementioned thermal bandwidth, the structure under study is subjected to an external transient load of 10 N at the free end for a duration of 1 ms. The control gain is calculated using negative velocity feedback algorithm, while the structural damping is taken to be 1 %. The beam displacement for both control on and control off are presented in Fig. 4. Seven different values of temperature $[-70, -50, -25, 0, 25, 50, 70]^\circ C$ have been tested. The results show that the efficiency of the piezoelectric layer on the control system is decreasing when the temperature is decreased, which agreed with the previous static analysis finding and can be explained by the fact that the piezoelectric coupling coefficient d_{31} is increasing proportionally with the temperature.

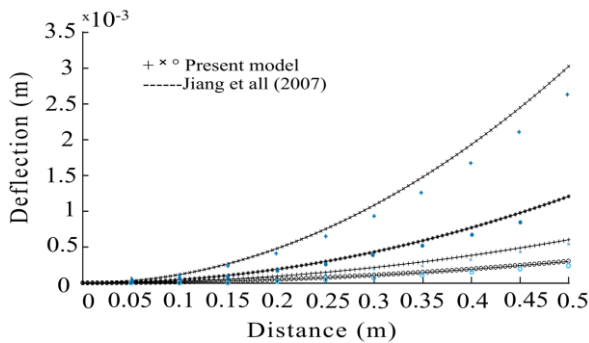


Fig. 2. Beam deflection along the length of the beam (+50°C, ● 20°C, * 10°C, ○ 5°C)

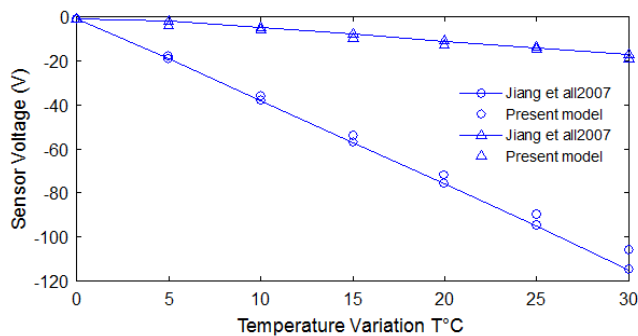


Fig. 3. Pzt sensor voltage due to temperature variation (o Thermal strain effect, Δ Pyroelectric effect)

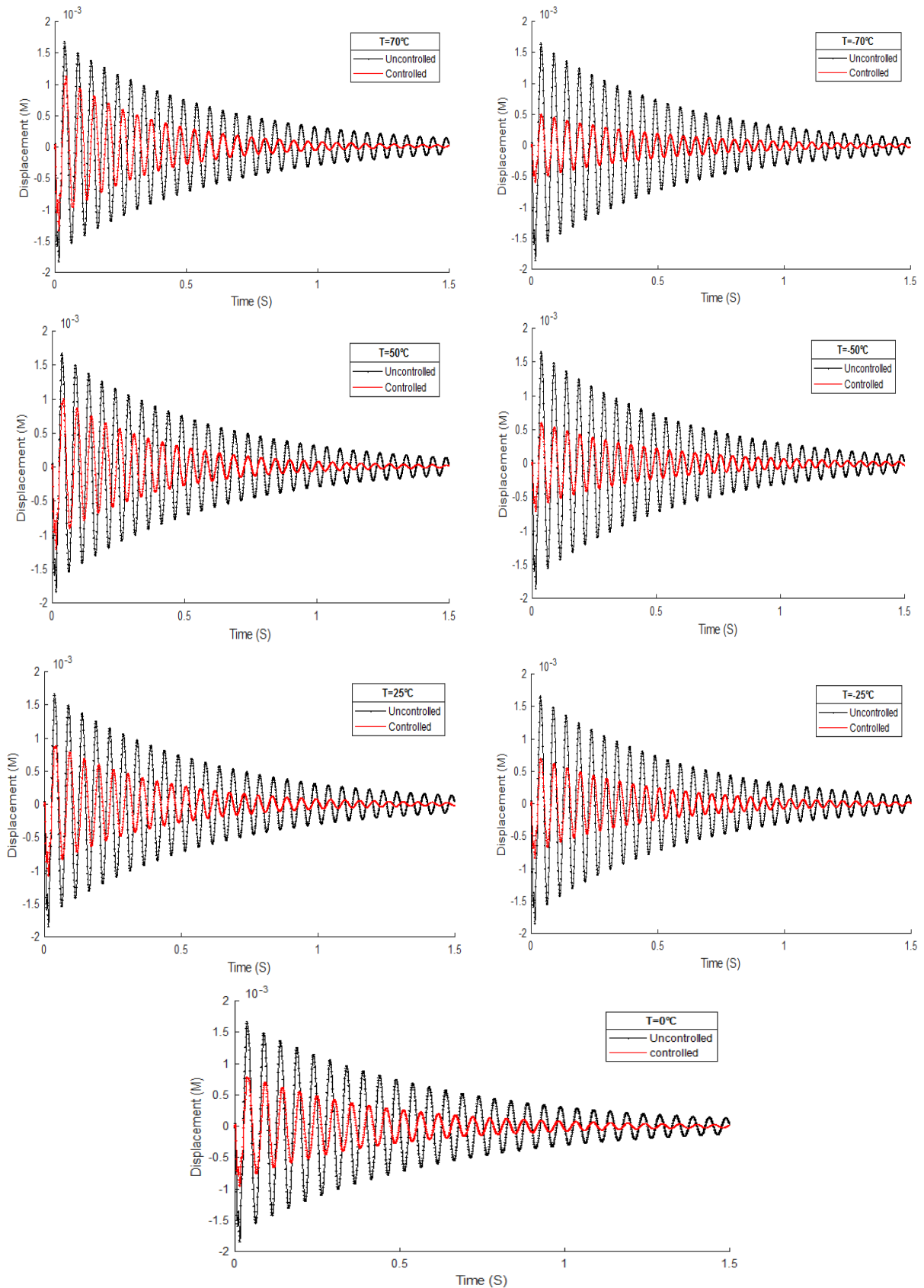


Fig. 4. Controlled dynamic response with a different thermal gradient (-70°C to 70°C)

The controlled and uncontrolled sensor signal at the previously mentioned temperature ranged is shown in Fig. 5. It can be observed that the sensor signal increase with temperature, which

proved the accuracy of the proposed control algorithm. The same control behavior as the displacement is noticed for the investigated temperature.

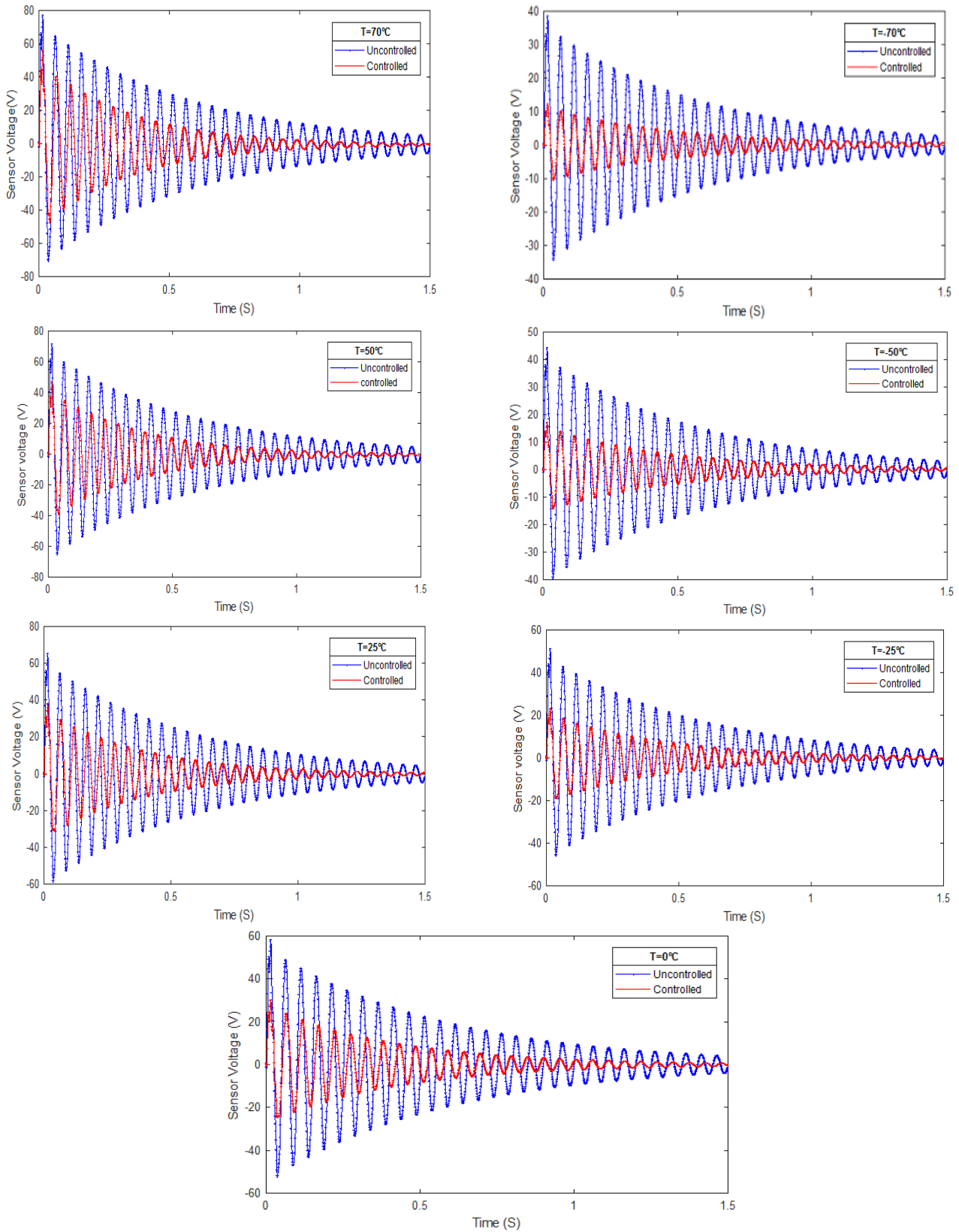


Fig. 5. Pzt sensor voltage due at different temperature

The actuator voltage with consideration of the range of temperature are depicted in Fig. 6. As it is clearly shown in the figure,

the actuator voltage is proportional to the temperature.

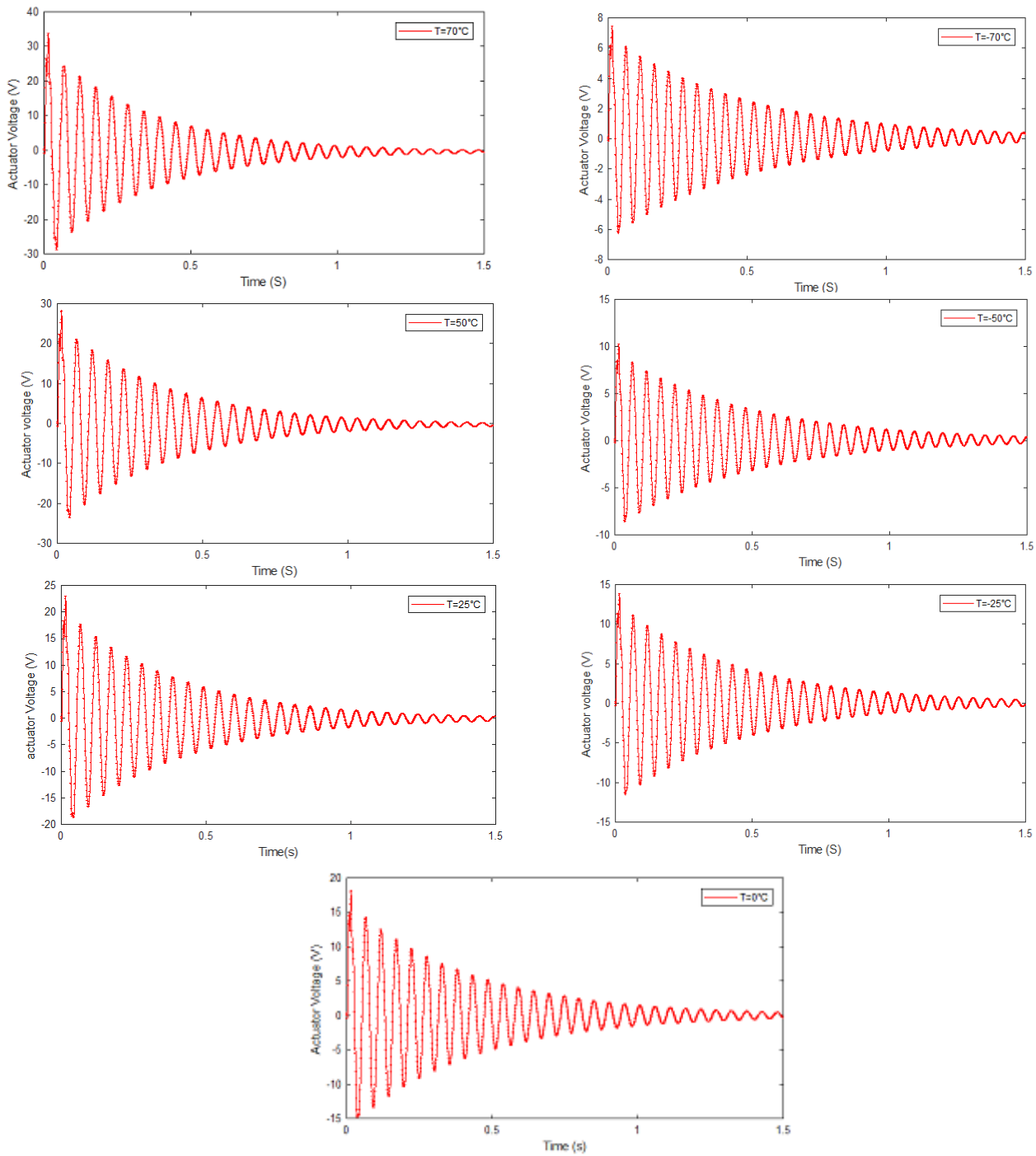


Fig. 6 Pzt actuator voltage versus time in different temperature 70°C, 50°C, 25°C, 0°C

8. CONCLUSION

In this paper, the finite element formulation for the laminated composite beam bounded by full recovery piezoelectric sensors and actuators has been developed for the purpose of AVC. The negative velocity feedback control algorithm is designed and implemented to provide the control gain. The coupling between thermal and piezoelectric effect is mathematically described and investigated. The results show a high dependency of the control efficiency on the temperature. The piezoelectric sensor voltage contributed by the thermal strain effect is much more than that contributed by pyroelectric effect. So, the temperature must be included in constitutive equations. It is found that AVC perfor-

mance is not maintained at a range of temperatures, if the control law ignores the temperature dependence of the PZT coefficients. However, AVC performance is maintained when the control law includes the temperature dependence of d_{31} and k_{33} . This scheme can be implemented in all the applications of smart structures where piezoelectric materials are used as sensors and actuators.

REFERENCES

1. **Bansal A., Ramaswamy A.** (2002), FE analysis of piezo-laminate composites under thermal loads, *J. Intell. Mater. Syst. Struct.*, 13,

- 291–301.
2. **Beheshti-Aval S.B., Lezgy-Nazargah M., Vidal P., Polit O.** (2011), A Refined Sinus Finite Element Model for the Analysis of Piezoelectric-Laminated Beams, A Refined Sinus Finite Element Model for the Analysis of Piezoelectric-Laminated Beams, *J. Intell. Mater. Syst. Struct.*, 22, 203–219, <https://doi.org/10.1177/1045389X10396955>.
 3. **Bendine K., Boukhoula F.B., Nouari M., Satla Z.** (2016), Active vibration control of functionally graded beams with piezoelectric layers based on higher order shear deformation theory, *Earthq. Eng. Eng. Vib.*, 15, 611–620.
 4. **Benjeddou A., Andrianarison O.** (2005), A thermopiezoelectric mixed variational theorem for smart multilayered composites, *Comput. Struct.*, 83, 1266–1276.
 5. **Birman V.** (1996), Thermal effects on measurements of dynamic processes in composite structures using piezoelectric sensors, *Smart Mater. Struct.*, 5, 379, <https://doi.org/10.1088/0964-1726/5/4/001>.
 6. **Chandrashekhara K., Tenneti R.** (1995), Thermally induced vibration suppression of laminated plates with piezoelectric sensors and actuators, *Smart Mater. Struct.*, 4, 281. <https://doi.org/10.1088/0964-1726/4/4/008>.
 7. **Chattopadhyay A., Li J., Gu H.** (1999), Coupled Thermo-Piezoelectric-Mechanical Model for Smart Composite Laminates, *AIAA J.*, 37, 1633–1638, <https://doi.org/10.2514/2.645>.
 8. **Clark W.W.** (1999), Semi-active vibration control with piezoelectric materials as variable-stiffness actuators, *Smart Structures and Materials: Passive Damping and Isolation*, International Society for Optics and Photonics, 123–130.
 9. **Crawley E.F., De Luis J.** (1987), Use of piezoelectric actuators as elements of intelligent structures, *AIAA J.*, 25, 1373–1385.
 10. **Elshafei M.A., Alraies F.** (2013), Modeling and analysis of smart piezoelectric beams using simple higher order shear deformation theory, *Smart Mater. Struct.*, 22, 035006.
 11. **Gay D., Hoa S.V.** (2007), *Composite Materials : Design and Applications*, Second Edition, CRC Press.
 12. **Gupta V., Sharma M., Thakur N., Singh S.P.** (2011), Active vibration control of a smart plate using a piezoelectric sensor–actuator pair at elevated temperatures, *Smart Mater. Struct.*, 20, 105023. <https://doi.org/10.1088/0964-1726/13/1/004> <https://doi.org/10.1115/1.3167719> <https://doi.org/10.1201/9781420045208>
 13. **Jiang J.P., Li D.X.** (2007), A new finite element model for piezothermoelastic composite beam, *J. Sound Vib.*, 306, 849–864.
 14. **Johnson C.D.** (1995), Design of Passive Damping Systems, *J. Mech. Des.*, 117, 171–176, <https://doi.org/10.1115/1.2836451>.
 15. **Kargarnovin M.H., Najafizadeh M.M., Viliani N.S.** (2007), Vibration control of a functionally graded material plate patched with piezoelectric actuators and sensors under a constant electric charge, *Smart Mater. Struct.*, 16, 1252.
 16. **Lam K.Y., Peng X.Q., Liu G.R., Reddy J.N.** (1997), A finite-element model for piezoelectric composite laminates, *Smart Mater. Struct.*, 6, 583.
 17. **Lee H.-J., Saravanos D.A.** (1996), Coupled layerwise analysis of thermopiezoelectric composite beams, *AIAA J.*, 34, 1231–1237.
 18. **Lee H.-J., Saravanos D.A.** (1998), The effect of temperature dependent material properties on the response of piezoelectric composite materials, *J. Intell. Mater. Syst. Struct.*, 9, 503–508.
 19. **Liew K.M., He X.Q., Ng T.Y., Sivashanker S.** (2001), Active control of FGM plates subjected to a temperature gradient: modelling via finite element method based on FSDT, *Int. J. Numer. Methods Eng.*, 52, 1253–1271.
 20. **Peng X.Q., Lam K.Y., Liu G.R.** (1998), Active vibration control of composite beams with piezoelectrics: a finite element model with third order theory., *J. Sound Vib.*, 209, 635–650.
 21. **Qiu J., Ji H., Zhu K.** (2009), Semi-active vibration control using piezoelectric actuators in smart structures, *Front. Mech. Eng. China*, 4, 242–251.
 22. **Raja S., Sinha P.K., Prathap G., Dwarakanathan D.** (2004), Thermally induced vibration control of composite plates and shells with piezoelectric active damping, *Smart Mater. Struct.*, 13, 939.
 23. **Reddy J.N.** (1984), A Simple Higher-Order Theory for Laminated Composite Plates, *J. Appl. Mech.*, 51, 745–752.
 24. **Sharma A., Kumar R., Vaish R., Chauhan V.S.** (2016), Experimental and numerical investigation of active vibration control over wide range of operating temperature, *J. Intell. Mater. Syst. Struct.*, 27, 1846–1860.
 25. **Song, G., Zhou, X., Binienda, W.** (2004), Thermal deformation compensation of a composite beam using piezoelectric actuators, *Smart Mater. Struct.*, 13, 30.
 26. **Tzou H.S., Bao Y.** (1995), A theory on anisotropic piezothermoelastic shell laminates with sensor/actuator applications, *J. Sound Vib.*, 184, 453–473.
 27. **Tzou H.S., Gadre M.** (1989), Theoretical analysis of a multi-layered thin shell coupled with piezoelectric shell actuators for distributed vibration controls, *J. Sound Vib.*, 132, 433–450.
 28. **Tzou H.S., Tseng C.I.** (1990), Distributed piezoelectric sensor/actuator design for dynamic measurement/control of distributed parameter systems: a piezoelectric finite element approach, *J. Sound Vib.*, 138, 17–34.
 29. **Wang D., Fotinich Y., Carman G.P.** (1998), Influence of temperature on the electromechanical and fatigue behavior of piezoelectric ceramics, *J. Appl. Phys.*, 83, 5342, <https://doi.org/10.1063/1.367362>.
 30. **Ye Z.-G.** (2008), *Handbook of advanced dielectric, piezoelectric and ferroelectric materials: Synthesis, properties and applications*, Elsevier.
 31. **Zhou X., Chattopadhyay A., Gu H.** (2000), Dynamic responses of smart composites using a coupled thermo-piezoelectric-mechanical model, *AIAA J.*, 38, 1939–1948.
 32. **Zorić N.D., Simonović A.M., Mitrović Z.S., Stupar S.N.** (2013), Optimal vibration control of smart composite beams with optimal size and location of piezoelectric sensing and actuation, *J. Intell. Mater. Syst. Struct.*, 24, 499–526.
 33. **Zou Y., Tong L., Steven G.P.** (2000), Vibration-based model-dependent damage (delamination) identification and health monitoring for composite structures — a review, *J. Sound Vib.*, 230, 357–378, <https://doi.org/10.1006/jsvi.1999.2624>.